

CHF model development for subcooled condition in narrow rectangular channel

Jung Hyun Song^{a*}, Jun Yeong Jung^a, Soon Heung Chang^b, Yong Hoon Jeong^{a*}

^aKorea Advanced Institute of Science and Technology, 373-1 Guseong-dong, Yuseong-gu, Daejeon 305-701, Republic of Korea

^bHandong University, 558 Handong-ro, Heunghae-eup, Book-gu, Pohang 37554, Republic of Korea

*Corresponding author: jeongyh@kaist.ac.kr

1. Introduction

Research reactors use plate-type fuel which has an advantage of higher ratio of heat transfer area to volume than rod-type fuel as shown in Fig. 1. From the geometrical characteristics, it has benefits on stronger resistance to external shock and power density in the core as well [1][2][3]. And they run under low pressure near the atmospheric condition with highly subcooled condition as they are usually open-pool type reactor and to avoid the boiling phenomena which can affect the intensity of neutron sources.

Due to the geometrical differences, the boiling phenomena in the narrow rectangular channel behave differently compared to that of circular tube. However, less researches had performed for narrow rectangular channel geometry. In addition, empirical correlations have limited use to assess the CHF performance over its validated range, especially for newly designed fuel geometries, thus, physical approach to investigate the CHF is desirable depending on flow conditions.

Several studies on the saturated flow CHF in the rectangular channel have been carried out based on annular flow regime [1][4][5]. In the contrast, CHF in subcooled flow boiling could be occurred slug flow, vapor clots, and even in bubbly flow [6] and no mechanistic approach was performed for subcooled flow in the narrow rectangular channel.

The purpose of this paper is subcooled CHF model in the narrow rectangular channel. The developed model was evaluated with CHF experimental data in the narrow rectangular channel from several studies considering various conditions, such as mass flux, inlet temperature and geometries. The pressure condition was less than 40 bar, relatively low pressure condition to consider the research reactor condition as explained above.

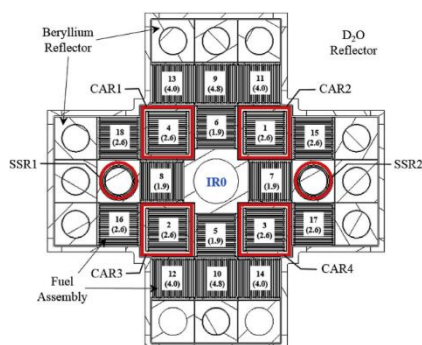


Fig. 1. Research reactor core layout [7]

2. Literature survey

Several studies have developed the mechanistic model to predict the CHF for subcooled flow boiling condition in the tube. Among various mechanisms of CHF, CHF due to dryout of liquid sublayer beneath the vapor blanket or slug bubble has been a basic CHF mechanism. The CHF is assumed to be occurred when the liquid sublayer is completely dried out before the coalesced bubble passes by.

Lee and Mudawwar (1988) proposed a mechanistic sublayer dryout model for high pressure conditions. They assumed the confined circumferential growth of vapor blanket and those bubbles prevent liquid entering the liquid sublayer from vapor blanket sides. Liquid sublayer thickness was calculated by a force balance on the vapor blanket in radial direction: vapor generation momentum and lateral force due to velocity gradient between two phases.

Katto (1990) suggested a model to predict the subcooled flow boiling CHF assuming homogeneous two-phase flow for extended pressure range: 1 – 200 bar. The author tenanted the liquid sublayer thickness suggested by Haramura and Katto (1983). Unlike Lee and Mudawwar (1988), the author calculated bubble velocity with an empirical correlations of velocity coefficient. This model has limitation that it cannot be applicable where the local void fraction exceeds 0.7.

Celata et al. (1994) assumed that coalesced vapor blanket can only exist in superheated layer in near-wall region. In this model, liquid sublayer thickness was determined by subtracting vapor blanket diameter from the superheated liquid layer thickness which was calculated by Martinelli temperature distribution [12].

Liu et al. (2000) postulated the critical wave lengths calculated by Helmholtz instability on both sides of vapor blanket are equal, then calculated the bubble velocity using two-phase average velocity and density. Then, the liquid sublayer thickness was figured out by subtracting the half of bubble diameter from the vapor blanket location calculated by Karman velocity distribution [14].

Liu et al. (2012) proposed a model which is very similar with Lee and Mudawwar (1988), but for both subcooled and saturated flow boiling CHF in motion conditions. The liquid sublayer thickness was computed not only with the evaporation momentum and the lateral

force but also with the radial buoyancy force and the wall lubrication force.

3. Model development

3.1 Assumptions

- (1) CHF is assumed to be occurred when the liquid sublayer beneath the vapor blankets is completely evaporated before the heated wall is replenished by surrounded liquid during the bubble passage time.
- (2) Vapor blanket velocity is determined by the local liquid velocity and the relative vapor blanket velocity.
- (3) Considering the geometrical characteristics of narrow rectangular channel, cross section of the test section is mostly occupied by coalesced bubble at CHF.
- (4) The length of vapor blanket is assumed to be same with the Helmholtz critical wavelength.

3.2 Constitutive equations

As mentioned above in the assumptions, the large coalesced bubble stretches into channel width direction by the channel confinement due to narrow gap and occupies most of cross section area as shown in Fig. 2. The coalesced bubble area is determined by the calculated void fraction during the calculation process.

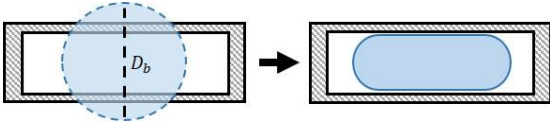


Fig. 2. Coalesced bubble shape in narrow rectangular channel

The coalesced bubble area and bubble diameter were calculated with the void fraction which was determined by true quality from Saha and Zuber [16]. True quality was calculated with equations (1) and (2). Void fraction was determined with equation (3).

$$\begin{cases} X_{\lambda} = -0.0022 \frac{q'' c_p D_e}{k_f h_{fg}} & \text{for } Pe < 70000 \\ X_{\lambda} = -153.8 \frac{q''}{G h_{fg}} & \text{for } Pe \geq 70000 \end{cases} \quad (1)$$

$$X_{true} = \frac{x_e - X_{\lambda} \exp\left(\frac{x_e - 1}{X_{\lambda}}\right)}{1 - X_{\lambda} \exp\left(\frac{x_e - 1}{X_{\lambda}}\right)} \quad (2)$$

$$\alpha = \frac{X_{true}}{C_0 \left(X_{true} \frac{\rho_f - \rho_g + \rho_g}{\rho_f} + 1.41 \frac{\rho_g}{G} \left(\frac{\sigma g (\rho_f - \rho_g)}{\rho_f^2} \right)^{0.25} \right)} \quad (3)$$

Where, $C_0 = 1.35 - 0.35 \sqrt{\frac{\rho_g}{\rho_f}}$ for rectangular channel

$$D_b = \sqrt{\frac{4}{\pi} a b \alpha} \quad (4)$$

With the coalesced bubble area, the drag coefficient was obtained from Harmathy [17] which was recommended for low pressure less than 10 bar.

$$C_D = \frac{2}{3} \frac{D_b}{\sqrt{\frac{\sigma}{g(\rho_f - \rho_g)}}} \quad (5)$$

Local liquid velocity was calculated by Karman velocity profile [14].

$$\begin{cases} U_{bL}^+ = y^+ & \text{for } 0 \leq y^+ < 5 \\ U_{bL}^+ = 5.0 \ln y^+ - 3.05 & \text{for } 5 \leq y^+ < 30 \\ U_{bL}^+ = 2.5 \ln y^+ + 5.5 & \text{for } y^+ \geq 30 \end{cases} \quad (6)$$

Where, $U_{bL}^+ = \frac{U_{bL}}{U_{\tau}}$, $U_{\tau} = \sqrt{\frac{\tau_w}{\rho_f}}$, $y^+ = y \frac{U_{\tau} \rho_f}{\mu_f}$, $\tau_w = \frac{f G^2}{2 \rho_f}$, $f = 0.079 Re^{-0.25}$

As reported in previous researches, the velocity of vapor blanket in the turbulent flow can be obtained by the force balance between buoyancy force and drag force on the vapor blanket.

$$\frac{\pi}{4} D_b^2 L_b g (\rho_f - \rho_g) = \frac{1}{2} \rho_f C_D (U_b - U_{bL})^2 \frac{\pi}{4} D_b^2 \quad (7)$$

$$U_b = \sqrt{\frac{2 L_b g (\rho_f - \rho_g)}{\rho_f C_D}} + U_{bL} \quad (8)$$

The length of vapor blanket was assumed to be same with Helmholtz instability of liquid-vapor interface. It was verified with the observed slug length in the experiments from Kinoshita et al. (1998).

$$L_b = \frac{2 \pi \sigma (\rho_f + \rho_g)}{\rho_f \rho_g U_b^2} \quad (9)$$

Liquid sublayer thickness beneath the vapor blanket or slug bubble was calculated from Haramura and Katto [10]. Dittus-Boelter correlation was utilized to predict single-phase heat transfer [19].

$$\delta_m = 0.0584^2 \frac{\pi}{2} \sigma \rho_g \left(\frac{\rho_g}{\rho_f} \right)^{0.4} \left(1 + \frac{\rho_g}{\rho_f} \right) \left(\frac{h_{fg}}{q_b''} \right)^2 \quad (10)$$

$$q_b'' = q_{CHF}'' - h_{f,single} (T_{sat} - T_o) \quad (11)$$

$$h_{f,single} = 0.023 Re^{0.8} Pr^{0.4} \frac{k_f}{D_e} \quad (12)$$

The critical heat flux was calculated by assuming that the minimum heat flux necessary to extinguish a liquid sublayer of liquid sublayer thickness by evaporation during the vapor blanket passage time with the bubble velocity and bubble length calculated above.

$$q_{CHF}'' = \frac{\rho_f \delta_m h_{fg} U_b}{L_b} \quad (13)$$

For a given geometric and inlet conditions, the CHF was calculated by an iterative procedure with the foregoing equations.

4. Results

The developed model and existing models were evaluated with the dataset by gathering the experimental CHF data from previous researches. The target condition is upward flow for subcooled boiling condition in narrow rectangular channel under low pressure.

The experimental conditions of used dataset was shown in Table 1.

Table 1. Experimental conditions of experimental dataset

	Yucel and Kakac (1978)	Kinoshita et al. (1998)	Tanaka et al. (2001)	Chang et al. (2002)	Kureta and Akimoto (2002)
Pressure (bar)	1.01	1.01	1.01	1.13	1.01
Mass flux (kg/m ² s)	1250 – 6250	2000 – 4000	1510 – 4007	1500 – 2000	853 – 15120
Quality	-0.072 – -0.008	-0.104 – -0.092	-0.089 – -0.035	-0.075 – -0.074	-0.125 – -0.006
Inlet subcooling (K)	8 – 45	60	80	50	10 – 70
Channel width (mm)	9.52	11	4	8	7 – 22
Channel gap (mm)	6.35	5	1.5	5	0.2 – 3
Heated length (mm)	305	50 – 80	98	100	50 – 200

Figs. 3 – 5 show the comparison of the dataset with predicted value assessed with existing models. Among these models, newly proposed model in this study showed the best prediction performance. Each model's prediction error is shown in Table 2.

Fig. 4 shows the predicted results with Katto model and it shows less number of data on the figure. The reason is that Katto model is not able to calculate the CHF for high void fraction condition which is over 70%. So, the predicted data whose void fraction is higher than 0.7 is excluded in the figure.

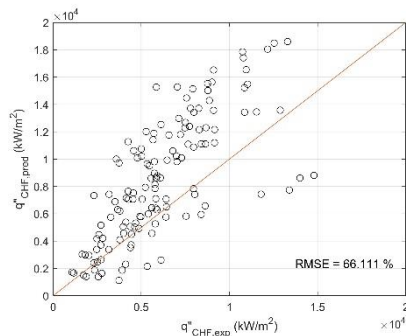


Fig. 3. M vs. P of CHF dataset (Celata et al., 1999)

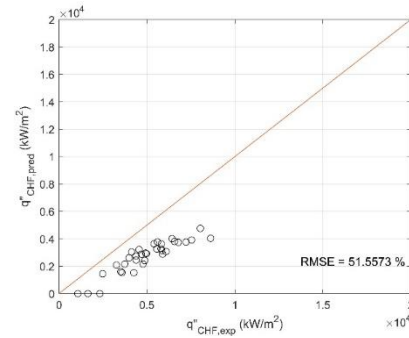


Fig. 4. M vs. P of CHF dataset (Katto, 1990)

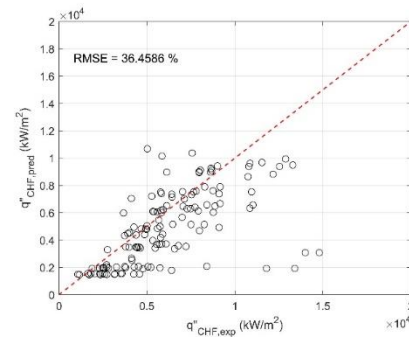


Fig. 5. M vs. P of CHF dataset (this study)

Table 2. Prediction performance of evaluated models

Model	Katto (1990)	Celata et al. (1999)	This study
RMS error	51.56 %	66.11 %	36.46 %

5. Conclusions

In the present study, new model was developed to predict the CHF for subcooled flow boiling condition in the narrow rectangular channel.

Nomenclature

a	channel width	(m)
b	channel gap	(m)
D_b	bubble diameter	(m)
D_e	equivalent diameter	(m)
G	mass flux	(kg/m ² s)
h_{fg}	latent heat of evaporation	(kJ/kg)
k_f	thermal conductivity	(kW/m K)
q''	heat flux	(kW/m ²)
T	temperature	(°C)
X_e	exit quality	(-)
ρ	density	(kg/m ³)
σ	surface tension	(N/m)
α	void fraction	(-)
δ	liquid sublayer thickness	(m)

Acknowledgement

This research was supported by the KAI-NEET Institute, KAIST, South Korea (N11200045).

REFERENCES

- [1] G. S. Choi, S. H. Chang, and Y. H. Jeong, "Prediction of the critical heat flux for saturated upward flow boiling water in vertical narrow rectangular channels," *Nucl. Eng. Des.*, vol. 303, pp. 1–16, Jul. 2016.
- [2] J. H. Song, J. Lee, and Y. H. Jeong, "Onset of Nucleate Boiling for Downward Flow in Narrow Rectangular Channel under Low Pressure," *Ann. Nucl. Energy*, vol. 109, no. 1980, pp. 1–12, 2017.
- [3] J. H. Song, J. Lee, S. H. Chang, and Y. H. Jeong, "Correction factor development for the 2006 Groeneveld CHF look-up table for rectangular channels under low pressure," *Nucl. Eng. Des.*, vol. 370, no. March, p. 110869, Dec. 2020.
- [4] D. X. Du, W. X. Tian, G. H. Su, S. Z. Qiu, Y. P. Huang, and X. Yan, "Theoretical study on the characteristics of critical heat flux in vertical narrow rectangular channels," *Appl. Therm. Eng.*, vol. 36, no. 1, pp. 21–31, 2012.
- [5] M. Gui, W. Tian, D. Wu, G. H. Su, and S. Qiu, "Study on CHF characteristics in narrow rectangular channel under complex motion condition," *Appl. Therm. Eng.*, vol. 166, no. July 2019, 2020.
- [6] J. M. Le Corre, S. C. Yao, and C. H. Amon, "Two-phase flow regimes and mechanisms of critical heat flux under subcooled flow boiling conditions," *Nucl. Eng. Des.*, vol. 240, no. 2, pp. 245–251, 2010.
- [7] K. O. Kim, B. J. Jun, B. Lee, S. J. Park, and G. Roh, "Comparison of first criticality prediction and experiment of the Jordan research and training reactor (JRTR)," *Nucl. Eng. Technol.*, vol. 52, no. 1, pp. 14–18, 2020.
- [8] C. H. Lee and I. Mudawwar, "A mechanistic critical heat flux model for subcooled flow boiling based on local bulk flow conditions," *Int. J. Multiph. Flow*, vol. 14, no. 6, pp. 711–728, 1988.
- [9] Y. Katto, "A physical approach to critical heat flux of subcooled flow boiling in round tubes," *Int. J. Heat Mass Transf.*, vol. 33, no. 4, pp. 611–620, 1990.
- [10] Y. Haramura and Y. Katto, "A new hydrodynamic model of critical heat flux, applicable widely to both pool and forced convection boiling on submerged bodies in saturated liquids," *Int. J. Heat Mass Transf.*, vol. 26, no. 3, pp. 389–399, 1983.
- [11] G. P. Celata, M. Cumo, A. Mariani, M. Simoncini, and G. Zummo, "Rationalization of existing mechanistic models for the prediction of water subcooled flow boiling critical heat flux," *Int. J. Heat Mass Transf.*, vol. 37, no. Supplement 1, pp. 347–360, 1994.
- [12] R. C. Martinelli, "Heat transfer to molten metals," *Trans. Am. Soc. Mech. Eng.*, vol. 69, pp. 947–959, 1947.
- [13] W. Liu, H. Nariai, and F. Inasaka, "Prediction of critical heat flux for subcooled flow boiling," *Int. J. Heat Mass Transf.*, vol. 43, no. 18, pp. 3371–3390, 2000.
- [14] T. von Kármán, "The analogy between fluid friction and heat transfer," *Trans. Am. Soc. Mech. Eng.*, vol. 61, pp. 705–710, 1939.
- [15] W. X. Liu *et al.*, "An improved mechanistic critical heat flux model and its application to motion conditions," *Prog. Nucl. Energy*, vol. 61, pp. 88–101, 2012.
- [16] P. Saha and N. Zuber, "Point of net vapor generation and vapor void fraction in subcooled boiling," *Proc. 5th Int. Heat Transf. Conf.*, no. May, pp. 175–179, 1974.
- [17] T. Z. Harmathy, "Velocity of large drops and bubbles in media of infinite or restricted extent," *AIChE J.*, vol. 6, no. 2, pp. 281–288, 1960.
- [18] H. Kinoshita, T. Yoshida, F. Inasaka, and H. Nariai, "Effect of Heated Length on the Critical Heat Flux of Subcooled Flow Boiling (1st report, observation of bubbles and slug length at atmospheric pressure)," *Nihon Kikai Gakkai Ronbunshu, B Hen/Transactions Japan Soc. Mech. Eng. Part B*, vol. 64, no. 624, pp. 2586–2593, 1998.
- [19] F. W. Dittus and L. M. K. Boelter, "University of California Publications on Engineering," *Univ. Calif. Publ. Eng.*, vol. 2, p. 371, 1930.
- [20] B. Yucel and S. Kakac, "forced flow boiling and burnout in rectangular channels," in *6th international heat transfer conference*, 1978, p. Vol. 1, 387-392.
- [21] F. Tanaka, T. Hibiki, Y. Saito, T. Takeda, and K. Mishima, "Heat transfer study for thermal-hydraulic design of the solid-target of spallation neutron source," *J. Nucl. Sci. Technol.*, vol. 38, no. 10, pp. 832–843, 2001.
- [22] S. H. Chang, I. C. Bang, and W. P. Baek, "A photographic study on the near-wall bubble behavior in subcooled flow boiling," *Int. J. Therm. Sci.*, vol. 41, no. 7, pp. 609–618, 2002.
- [23] M. Kureta and H. Akimoto, "Critical heat flux correlation for subcooled boiling flow in narrow channels," *Int. J. Heat Mass Transf.*, vol. 45, no. 20, pp. 4107–4115, 2002.
- [24] G. P. Celata, M. Cumo, Y. Katto, and A. Mariani, "Prediction of the critical heat flux in water subcooled flow boiling using a new mechanistic approach," *Int. J. Heat Mass Transf.*, vol. 42, no. 8, pp. 1457–1466, 1999.